Interaction Notes

Note 194

August 1974

Relationship Between Total Currents and Surface Current Densities Induced on Aircraft and Cylinders

by

M. I. Sancer
R. W. Latham
A. D. Varvatsis

Tetra Tech, Inc.
Pasadena, California

Several discrepancies are discussed, both qualitatively and quantitatively, concerning procedures of obtaining surface current densities from total currents. It is shown that for frequencies corresponding to a large portion of an EMP spectrum, significant errors are made by inferring surface current densities from a calculated total current. This has important implications in that it is surface current densities that are required in order to calculate the currents induced on cables within the structure.

I. LOW FREQUENCY SURFACE CURRENT DISTRIBUTIONS ON AIRCRAFT

In determining the EMP interaction with systems within an aircraft, a wire model of the aircraft is often assumed [1]. This model often assumes a single straight wire to model the aircraft fuselage and other straight wires to model the wings and tail structure [2]. In working with wire models one can at best predict total currents flowing along the various wires. Since the EMP interaction with systems within the aircraft is dominated by aperture coupling through the various ports of entry, what is really needed is the surface current distribution. The usual way of connecting the total currents predicted by the wire model with the required surface current is to assume a uniform current distribution around the various aircraft elements modeled by the straight wires (a more sophisticated version of this assumption is to distribute the surface current according to the simplest static solution carrying the same net current on an infinite cylinder of the same cross-section shape [3]). There is undoubtedly a range of frequencies where this approach is adequate. But clearly, at wavelengths short enough that a half wavelength becomes comparable to the diameter of, say, the fuselage, the wire model is inadequate to predict surface currents since surface current then tends to concentrate on the side from which the energy is incident as can be seen from an infinite cylinder analysis. ([4] fig 2. 3). Another study of a finite hollow cylinder also shows a shadowing effect for moderately high frequencies [5]. It is not so clear, initially, that the wire model approach also breaks down at low frequencies, but this fact also becomes obvious after a few elementary quasistatic calculations. Since a significant portion of the EMP energy occurs in what we have called the low frequencies it is worthwhile to bring attention to these quasistatic calculations in this note.

The basic reason that the wire model approach breaks down at low frequencies is that the currents predicted by using such a model are really those currents associated with charge transport. The circulating surface currents associated with the interaction of the aircraft with the magnetic field of the incident wave are neglected (this separation of the effect of the magnetic field interaction from the electric field interaction is only possible in the low frequency quasistatic regime). As a preliminary estimate of the effect of the quasistatic magnetic field in inducing surface currents, we can note that if we have an infinite circular cylinder of radius a, whose axis is the z-axis of a Cartesian coordinate system, immersed in an incident wave propagating parallel to the x-axis we have, if the incident H field is in the negative y direction, a magnetostatic surface current of the form [6]

$$\underline{K} = 2\underline{e}_z H_o \cos \varphi \tag{1}$$

where H_o is the magnitude of the incident field and $\varphi = \tan^{-1}(y/x)$. For a really infinite cylinder this surface current is dominated by the uniformly distributed surface current associated with charge transport, which diverges like $(\omega \ln \omega)^{-1}$ at low frequency, but this charge transport current really approaches zero in proportion to ω at low frequency, if the cylinder is of finite length, while the magnetically induced current is still approximately given by equation (1), if one stays a few radii away from the end of the cylinder.

The other case of incident wave polarization on an infinite cylinder, where the incident H field is parallel to the cylinder, demonstrates a more clean-cut case of the inadequacy of wire models in predicting surface currents. In such a case the wire model current is zero (the electric field is everywhere perpendicular to the wire so there is no forcing function in the wire-current integral equation). This is true in the sense that there really is no z-directed current, but there is a circulating current equal in magnitude to the incident H field [6].

The infinite cylinder results are a little unsatisfactory in that we had to say the charge transport current goes to zero at low frequency by making the cylinder finite in an ad hoc manner. A more convincing argument for the importance of magnetically induced currents can be made by looking at the prolate spheroid, which can also be treated in an elementary analytical manner. For the prolate spheroid it is obvious that the charge-transport current goes to zero at low frequency.

The magnetically induced surface currents can be calculated by solving an appropriate magnetostatic problem. Let the axis of the spheroid lie along the z-axis of a Cartesian coordinate system and the incident H-field be in the negative y direction. By introducing a magnetostatic potential, Ω, we can reduce flow of an ideal fluid and use reference [7] (p. 535, eq. 4) to say that the total potential, on the surface of the spheroid, is given by

$$\Omega_T = H_o\, y\left(\frac{2}{2-\alpha_o}\right) \tag{2}$$

where, if a and b are the semimajor and semiminor axes of the ellipse, respectively, we have

$$\alpha_o = ab^2 \int_o^{\infty} \frac{d\lambda}{(b^2+\lambda)^2\sqrt{a^2+\lambda}} \tag{3}$$

The integration defining α_o can be performed in an elementary way ([8] nos. 105 and 103) to obtain

$$\alpha_o = \frac{1}{1-\varepsilon^2}\left\{1 + \frac{\varepsilon^2}{2\sqrt{1-\varepsilon^2}} \ln\left(\frac{1-\sqrt{1-\varepsilon^2}}{1+\sqrt{1-\varepsilon^2}}\right)\right\} \tag{4}$$

where $\varepsilon = b/a$. If $\varepsilon = .1$, we have α_o equal to .9797 and Ω_T, from equation 2, given by

$$\Omega_T = 1.96\ H_o y \tag{5}$$

We can calculate the surface current from this expression by forming $-\underline{n} \times \nabla_s \Omega_T$ where $\underline{n}$ is the outward normal from the spheroid and ∇_s denotes a surface gradient. The surface current has various components, but at the central cross-section it is given by

$$\underline{K} = 1.96\ \underline{e}_s \cos\varphi \tag{6}$$

i.e., within 2% of equation (1). This result is also in excellent agreement with the results presented for a finite cylinder contained in a subsequent section of this note.

There may be an objection to the type of calculation given above because it is based on perfect conductivity at low frequency. Since at d.c. the magnetic field penetrates the aircraft almost completely, one might ask how high in frequency one has to go in order for the perfect conductivity assumption to be reasonable. The answer to this question is given in reference [6] where it is shown that as long as $\omega \mu_0 \sigma \Delta b$ is much greater than unity the above calculated current distributions are accurate, where σ and Δ are the conductivity and wall thickness of the aircraft (prolate spheroid) and b is the radius (semiminor axis). At the same time we must have a frequency low enough so that the length of the spheroid is a small fraction of a wavelength in order for the quasistatic approach to be valid. Is there a frequency region where both conditions are met? Yes indeed, in fact, assuming reasonable physical parameters, the approach is valid for $100 < f < 10^6$, a rather wide range.

All in all, it is clear that the wire model approach to surface current prediction is inadequate at low frequencies as well as at high frequencies.

II. PROOF THAT AT LOW FREQUENCIES THE CURRENTS INDUCED ON A FINITE CYLINDER ARE NOT UNIFORM

Consider the following situation concerning the cylinder depicted in figure 1

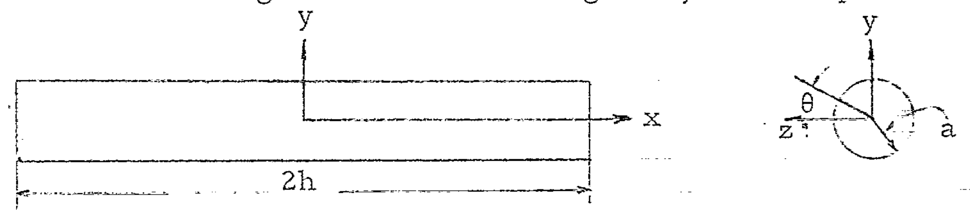

FIGURE 1

with incident magnetic field given by

$$\underline{H}_i = -\hat{a}_y e^{-ikz} \tag{7}$$

The usual magnetic field integral equation is given by

$$\tfrac{1}{2}\underline{J}(\underline{r}) = \underline{J}_i(\underline{r}) + \int_S \underline{\underline{K}}(\underline{r}, \underline{r}_o) \cdot \underline{J}(\underline{r}_o)\, dS_o \tag{8}$$

where S is the total surface of the cylinder. We now break up the total surface S into two surfaces S_+ and S_- where the + and - sign correspond to the sign of z. We also designate radius vectors $\underline{r}$ and $\underline{r}_o$ as $\underline{r}^+$, $\underline{r}_o^+$, $\underline{r}^-$, and $\underline{r}_o^-$ according to the sign of the z component of these vectors. We now rewrite (8)

$$\tfrac{1}{2}\underline{J}(\underline{r}^+) = \underline{J}_i(\underline{r}^+) + \int_{S_+} \underline{\underline{K}}(\underline{r}^+, \underline{r}_o^+) \cdot \underline{J}(\underline{r}_o^+)\, dS_o + \int_{S_-} \underline{\underline{K}}(\underline{r}^+, \underline{r}_o^-) \cdot \underline{J}(\underline{r}_o^-)\, dS_o \tag{9}$$

and

$$\tfrac{1}{2}\underline{J}(\underline{r}^-) = \underline{J}_i(\underline{r}^-) + \int_{S_+} \underline{\underline{K}}(\underline{r}^-, \underline{r}_o^+) \cdot \underline{J}(\underline{r}_o^+)\, dS_o + \int_{S_-} \underline{\underline{K}}(\underline{r}^-, \underline{r}_o^-) \cdot \underline{J}(\underline{r}_o^-)\, dS_o \tag{10}$$

In order to decompose these equations into symmetric and antisymmetric parts we introduce the reflection operator

$$\underline{\underline{R}}_1 = \underline{\underline{I}} - 2\hat{a}_z \hat{a}_z \tag{11}$$

where $\underline{\underline{I}}$ is the unit dyadic. We also introduce the notation

$$\underline{\underline{R}}_1 \cdot \underline{J}(\underline{r}_o^-) = \underline{\underline{R}}_1 \cdot \underline{J}(\underline{\underline{R}}_1 \cdot \underline{r}^+) \equiv \underline{J}^*(\underline{r}^+) \tag{12}$$

Using the fact that

$$\underline{\underline{R}}_1 \cdot \underline{\underline{R}}_1 = \underline{\underline{I}} \tag{13}$$

and scalar multiplying (10) by $\underline{\underline{R}}_1$, we obtain

$$\tfrac{1}{2}\underline{J}(\underline{r}^+) = \underline{J}_i(\underline{r}^+) + \int_{S_+} \underline{\underline{K}}(\underline{r}^+, \underline{r}_o^+) \cdot \underline{J}(\underline{r}_o^+)\, dS_o + \int_{S_+} \underline{\underline{K}}(\underline{r}^+, \underline{\underline{R}}_1 \cdot \underline{r}_o^+) \cdot \underline{\underline{R}}_1 \cdot \underline{J}^*(\underline{r}_o^+)\, dS_o \tag{14}$$

$$\tfrac{1}{2}\underline{J}^*(\underline{r}^+) = \underline{\underline{R}}_1 \cdot \underline{J}_i(\underline{\underline{R}}_1 \cdot \underline{r}^+) + \int_{S_+} \underline{\underline{R}}_1 \cdot \underline{\underline{K}}(\underline{\underline{R}}_1 \cdot \underline{r}^+, \underline{r}_o^+) \cdot J(\underline{r}_o^+)\, dS_o + \int_{S_+} \underline{\underline{R}}_1 \cdot \underline{\underline{K}}(\underline{\underline{R}}_1 \cdot \underline{r}^+, \underline{\underline{R}}_1 \cdot \underline{r}^+) \cdot \underline{\underline{R}}_1\, J^*(\underline{r}_o^+)\, dS_o \tag{15}$$

Recalling that $\underline{\underline{K}}(\underline{r}, \underline{r}_o) = \hat{n} \times [\nabla G_o \times \underline{\underline{I}}]$, the following relations can be proved

$$\underline{\underline{K}}(\underline{r}^+, \underline{r}_o^+) = \underline{\underline{R}}_1 \cdot \underline{\underline{K}}(\underline{\underline{R}}_1 \cdot \underline{r}^+, \underline{\underline{R}}_1 \cdot \underline{r}_o^+) \cdot \underline{\underline{R}}_1 \equiv \underline{\underline{A}}(\underline{r}^+, \underline{r}_o^+) \tag{16}$$

and

$$\underline{\underline{K}}(\underline{r}^+, \underline{\underline{R}}_1 \cdot \underline{r}_o^+) \cdot \underline{\underline{R}}_1 = \underline{\underline{R}}_1 \cdot \underline{\underline{K}}(\underline{\underline{R}}_1 \cdot \underline{r}^+, \underline{r}_o^+) \equiv \underline{\underline{B}}(\underline{r}^+, \underline{r}_o^+) \tag{17}$$

Substituting (16) and (17) into (14) and (15) and then adding and subtracting the resulting equations we obtain are

$$\tfrac{1}{2}\underline{J}^+(\underline{r}^+) = \underline{J}_i^+(\underline{r}^+) + \int_{S_+} \underline{\underline{K}}^+(\underline{r}^+, \underline{r}_o^+) \cdot \underline{J}^+(\underline{r}_o^+)\, dS_o \tag{18}$$

and

$$\tfrac{1}{2}\underline{J}^-(\underline{r}^+) = \underline{J}_i^-(\underline{r}^+) + \int_{S_+} \underline{\underline{K}}^-(\underline{r}^+, \underline{r}_o^+) \cdot \underline{J}^-(\underline{r}_o^+)\, dS_o \tag{19}$$

where

$$\underline{J}^+(\underline{r}^+) = \tfrac{1}{2}[\underline{J}(\underline{r}^+) + J^*(\underline{r}^+)] \tag{20}$$

$$\underline{J}^-(\underline{r}^+) = \tfrac{1}{2}[\underline{J}(\underline{r}^+) - \underline{J}^*(\underline{r}^+)] \tag{21}$$

$$\underline{J}_i^+(\underline{r}^+) = \tfrac{1}{2}[\underline{J}_i(\underline{r}^+) + \underline{\underline{R}}_1 \cdot \underline{J}_i(\underline{\underline{R}}_1 \cdot \underline{r}^+)] \tag{22}$$

$$\underline{J}_i^-(\underline{r}^+) = \tfrac{1}{2}[\underline{J}_i(\underline{r}^+) - \underline{\underline{R}}_1 \cdot \underline{J}_i(\underline{\underline{R}}_1 \cdot \underline{r}^+)] \tag{23}$$

$$\underline{\underline{K}}^+(\underline{r}^+, \underline{r}_o^+) = \underline{\underline{A}}(\underline{r}^+, \underline{r}_o^+) + \underline{\underline{B}}(\underline{r}^+, \underline{r}_o^+) \tag{24}$$

$$\underline{\underline{K}}^-(\underline{r}^+, \underline{r}_o^+) = \underline{\underline{A}}(\underline{r}^+, \underline{r}_o^+) - \underline{\underline{B}}(\underline{r}^+, \underline{r}_o^+) \tag{25}$$

Once we have determined $\underline{J}^+(\underline{r}^+)$ and $\underline{J}^-(\underline{r}^+)$ we can determine the current density on the +z and -z portion of the cylinder as follows

$$\underline{J}(\underline{r}^+) = \underline{J}^+(\underline{r}^+) + \underline{J}^-(\underline{r}^+) \tag{26}$$

and

$$\underline{J}(\underline{\underline{R}}_1 \cdot \underline{r}^+) = \underline{\underline{R}}_1 \cdot [\underline{J}^+(\underline{r}^+) - \underline{J}^-(\underline{r}^+)] \tag{27}$$

Noting that the unit vector in the longitudinal direction is $\hat{a}_x$, we see that

$$\hat{a}_x \cdot \underline{J}(r^+) = \hat{a}_x \cdot \underline{J}^+(\underline{r}^+) + \hat{a}_x \cdot \underline{J}^-(\underline{r}^+) \tag{28}$$

$$\hat{a}_x \cdot \underline{J}(\underline{\underline{R}}_1 \cdot \underline{r}^+) = \hat{a}_x \cdot \underline{J}^+(\underline{r}^+) - \hat{a}_x \cdot \underline{J}^-(\underline{r}^+) \qquad (29)$$

Next we will argue that

$$\lim_{k \to 0} \underline{J}_i^+(\underline{r}^+) = 0 \qquad (30)$$

If (30) is true, then it follows from the uniqueness of a solution to (18) that

$$\lim_{k \to 0} \underline{J}^+(\underline{r}^+) = 0 \qquad (31)$$

From (28), (29), and (31) it follows for small k that

$$\hat{a}_x \cdot \underline{J}(\underline{r}^+) \approx - \hat{a}_x \cdot \underline{J}(\underline{r}^-) \qquad (32)$$

which shows that the variation about the cylinder is anything but uniform as has sometimes previously been assumed. In order to show (30), we look at the explicit expressions for the source term. Recalling that $\underline{J}_i = \hat{n} x \underline{H}_i$ with $\underline{H}_i$ given in (7) and using the fact that

$$\underline{\underline{R}}_1 \cdot \left[\hat{n}(\underline{\underline{R}}_1 \cdot \underline{r}^+) \times \hat{a}_y \right] = -\hat{n}(\underline{r}^+) \times \hat{a}_y$$

we can write the explicit expressions for $\underline{J}_i^+(\underline{r}^+)$ and $\underline{J}_i^-(\underline{r}^+)$ given in (22) and (23) as

$$\underline{J}_i^+(\underline{r}^+) = [\hat{n}(\underline{r}^+) \times \hat{a}_y] \, (i \sin kz) \qquad (33a)$$

and similarly

$$\underline{J}_i^-(\underline{r}^+) = [\hat{n}(\underline{r}^+) \times \hat{a}_y] \, (-\cos kz) \qquad (33b)$$

From (33a) we see that the limit expressed in (30) is true and consequently so is the surprising relation given in (32) which was the statement to be proved.

III. NUMERICAL ERROR IN ASSUMMING THAT THE LONGITUDINAL CURRENT DENSITY IS UNIFORM

We have made calculations for the following geometry depicted in figure 1 where the incident field is given by

$$\underline{H}_{inc} = -H_o \hat{a}_y e^{-ikz}$$

We have chosen the cylinder to have dimensions $a/h = .1$ so that except for a relabeling of coordinates we have the same situation described in [9], figure 2. We now define three quantities that we have calculated with our new computer code.

$$J_f = J_x/hH_o \quad (x = h/10, \ \theta = 45^\circ) \tag{34}$$

$$J_b = J_x/hH_o \quad (x = h/10, \ \theta = 135^\circ) \tag{35}$$

If the field were uniform, independent of θ, then $J_f = J_b = J_{old}$

where

$$J_{old} = (I/2\pi a)/hH_o \tag{36}$$

Our results show that for frequencies corresponding to a significant portion of the EMP spectrum $J_f \neq J_b \neq J_{old}$, and the use of J_{old} rather than J_f and J_b for the calculation of interior cable currents is very inaccurate.

kh	h = 5m f(MHz)	h = 10m f(MHz)	h = 20m f(MHz)	** $Re(J_f)$	*** $Im(J_f)$	$Re(J_b)$	$Im(J_b)$	$Re(J_{old})$	$Im(J_{old})$	*% error (front)
.025	.24	.12	.06	1.41	-.079	-1.41	-.079	~0	-.079	99+
.05	.48	.24	.12	1.41	-.159	-1.41	-.159	~0	-.159	99+
.075	.72	.36	.18	1.41	-.239	-1.41	-.239	~0	-.239	98+
.1	.95	.48	.24	1.41	-.319	-1.41	-.319	~0	-.319	97+
.2	1.91	.95	.48	1.41	-.651	-1.41	-.651	~0	-.651	90+
.3	2.86	1.43	.72	1.41	-1.01	-1.40	-1.01	.005	-1.01	81+
.4	3.82	1.91	.95	1.42	-1.41	-1.39	-1.41	.015	-1.41	70+
.5	4.77	2.39	1.19	1.45	-1.88	-1.36	-1.87	.045	-1.88	59+
.6	5.73	2.86	1.43	1.51	-2.44	-1.29	-2.44	.109	-2.44	49+
.7	6.68	3.34	1.67	1.64	-3.14	-1.15	-3.14	.246	-3.14	40+
.8	7.64	3.82	1.91	1.93	-4.05	-.862	-4.05	.533	-4.05	32+
1	9.55	4.77	2.39	3.87	-6.71	1.10	-6.69	2.49	-6.70	20+

*% error (front) $\dfrac{|J_f - J_{old}|}{|J_f|} \times 100$

**Re( ) corresponds to the real part of ( )

***Im( ) corresponds to the imaginary part ( )

IV. EFFECT ON THE CALCULATION OF INTERIOR CABLE CURRENTS

According to [10] there are two types of equivalent sources used to calculate voltages and currents generated on cables internal to a cylindrical portion of conducting body containing "small" apertures, when the body is exposed to an incident EMP. For most bodies of interest, all apertures are "small" compared to the surrounding geometry as well as the wavelengths corresponding to most of the EMP spectrum. The equations that describe the voltage and current at any point on an interior cable are

$$V_{int} = AV_{eq} + BI_{eq} \tag{37}$$

$$I_{int} = CV_{eq} + DI_{eq} \tag{38}$$

where A, B, C, D depend on the internal geometry and termination of the cable. It is important to realize that

$$V_{eq} = K_v J_t \tag{39}$$

and

$$I_{eq} = K_I \nabla_s \cdot J \tag{40}$$

where K_v and K_I depend on the shape of the aperture and the internal geometry; however, J_t and $\nabla_s \cdot J$ are calculated as though the body contained no aperture. It is important to note that K_v also is proportional to frequency. Specifically, $\underline{J}$ is the total surface current <u>density</u> induced on the body and is given by

$$\underline{J} = J_s \hat{s} + J_t \hat{t} \tag{41}$$

where $\hat{t}$ is defined along the axis of the cylindrical portion of the body while $\hat{s}$ is the other orthogonal surface tangential vector chosen so that $\hat{s} \times \hat{t} = \hat{n}$ (the outward normal to the body).

It is important to stress that the main output of previous computer codes yields the total axial current I, and it is assumed that

$$J_t = I/2\pi a$$

where a is the radius of the cylinder. In the previous section we showed that this calculation is highly in error; however, it should be mentioned that the effect of this error is diminished by the frequency dependence of K_v. Also, we note that there is not even a procedure for obtaining J_s from I, and from (40) we see that $\nabla_s \cdot J_s = \nabla_s \cdot [J_s \hat{s} + J_t \hat{t}]$ is necessary to obtain I_{eq}. It is now apparent that a knowledge of the total current I induced on the exterior of a structure is insufficient to calculate the voltages and currents on cables within the structure. This conclusion has implications for all methods used to calculate the total current. Specifically, the integral equation method as well as the SEM method must be employed in a manner to obtain surface current densities rather than the total current.

ACKNOWLEDGEMENT

We thank Scott Siegel for his help in performing the necessary computer programming. We also thank Carl Baum, Phil Castillo, and Mike Harrison for their interest and support of this work.

REFERENCES

[1] Clayborne D. Taylor, Terry T. Crow, "Induced electric current on some configurations of wires, Part I, perpendicular crossed wires," EMP Interaction Notes, IN 85, Nov. 1971.

[2] Terry T. Crow, Thomas H. Shumpert, Clayborne D. Taylor, "Induced electric current on some configuration of wires, Part II, nonperpendicular intersecting wires," EMP Interaction Notes, IN 100, Apr. 1972.

[3] F. M. Tesche, "Charge distribution on a two-dimensional air-foil," EMP Interaction Notes, IN 75, May 1971.

[4] J. J. Bowman, T. B. A. Senior, P. L. E. Usleghi, editors, Electromagnetic and Acoustic Scattering by Simple Shapes, North-Holland, New York, 1969.

[5] C. W. Harrison, Jr., "Missile circumferential current density for plane wave electromagnetic field illumination," EMP Interaction Notes, IN 60, July 1970.

[6] R. W. Latham and K. S. H. Lee, "Theory of inductive shielding," EMP Interaction Notes, IN 12, March 1968.

[7] L. M. Milne-Thompson, Theoretical Hydrodynamics, Fifth edition, The Macmillan Co., New York, 1968.

[8] B. D. Pierce, Ronald M. Foster, A Short Table of Integrals, Ginn and Co., New York, 1956.

[9] R. W. Sassman, "The current induced on a finite, perfectly conducting, solid cylinder in free space by an electromagnetic pulse," EMP Interaction Notes, IN 11, July 1967.

[10] R. W. Latham, "Small holes in cable shields," EMP Interaction Notes, IN 118, September 1972.